World Academy of Science, Engineering and Technology
International Journal of Architectural and Environmental Engineering
Vol:11, No:4, 2017

Dynamic High-Rise Moment Resisting Frame Dissipation Performances Adopting Glazed Curtain Walls with Superelastic Shape Memory Alloy Joints

Lorenzo Casagrande, Antonio Bonati, Ferdinando Auricchio, Antonio Occhiuzzi

Open Science Index, Architectural and Environmental Engineering Vol:11, No:4, 2017 publications.waset.org/10006834.pdf

***Abstract*—**This paper summarizes the results of a survey on smart non-structural element dynamic dissipation when installed in modern high-rise mega-frame prototypes. An innovative glazed curtain wall was designed using Shape Memory Alloy (SMA) joints in order to increase the energy dissipation and enhance the seismic/wind response of the structures. The studied buildings consisted of thirty- and sixty-storey planar frames, extracted from reference three-dimensional steel Moment Resisting Frame (MRF) with outriggers and belt trusses. The internal core was composed of a CBF system, whilst outriggers were placed every fifteen stories to limit second order effects and inter-storey drifts. These structural systems were designed in accordance with European rules and numerical FE models were developed with an open-source code, able to account for geometric and material nonlinearities. With regard to the characterization of non-structural building components, full-scale crescendo tests were performed on aluminium/glass curtain wall units at the laboratory of the Construction Technologies Institute (ITC) of the Italian National Research Council (CNR), deriving force-displacement curves. Three-dimensional brick-based inelastic FE models were calibrated according to experimental results, simulating the façade response. Since recent seismic events and extreme dynamic wind loads have generated the large occurrence of non-structural components failure, which causes sensitive economic losses and represents a hazard for pedestrians safety, a more dissipative glazed curtain wall was studied. Taking advantage of the mechanical properties of SMA, advanced smart joints were designed with the aim to enhance both the dynamic performance of the single non-structural unit and the global behavior. Thus, three-dimensional brick-based plastic FE models were produced, based on the innovated non-structural system, simulating the evolution of mechanical degradation in aluminium-to-glass and SMA-to-glass connections when high deformations occurred. Consequently, equivalent nonlinear links were calibrated to reproduce the behavior of both tested and smart designed units, and implemented on the thirty- and sixty-storey structural planar frame FE models. Nonlinear time history analyses (NLTHAs) were performed to quantify the potential of the new system, when considered in the lateral resisting frame system (LRFS) of modern high-rise MRFs. Sensitivity to the structure height was explored comparing the responses of the two prototypes. Trends in global and local performance were discussed to show that, if accurately designed, advanced materials in non-structural elements provide new sources of energy dissipation.

***Keywords*—**Advanced technologies, glazed curtain walls, non-structural elements, seismic-action reduction, shape memory alloy.

Lorenzo Casagrande is with the Construction Technologies Institute (ITC) of the National Research Council (CNR), MI 20098 Italy (phone: +39 029806428; e-mail: Casagrande@itc.cnr.it) and with the Civil Engineer and Architectural Department, University of Pavia (e-mail: lorenzo.casagrande01@universitadipavia.it).

Antonio Bonati is with the Construction Technologies Institute (ITC) of the National Research Council (CNR), MI 20098 Italy (phone: +39 029806306; e-mail: Bonati@itc.cnr.it).

Ferdinando Auricchio is with the Civil Engineer and Architectural Department, University of Pavia, Pavia, PV 27100 Italy (phone: +39 0382 985476; e-mail: auricchio@unipv.it).

Antonio Occhiuzzi is the Director of Construction Technologies Institute (ITC) of the National Research Council (CNR), MI 20098 Italy (phone: +39 029806417; e-mail: Occhiuzzi@itc.cnr.it).

I. Introduction

MODERN computational tools, innovative construction techniques, high-strength and smart materials, have redefined the skyline of the most populated cities. Tall, supertall, and megatall buildings have become common concepts in architecture and engineering, facing the scarcity of land and mitigating the growing need for residential and business space [1]-[3]. However, the height request ensured the cost effectiveness achievement only through adequate technological improvements, aimed to revolutionary industrial production. Moreover, inappropriate ground typologies in severe seismicity areas and wind dynamic excitation, could aggravate intrinsic complex features strictly related to structural large dimensions [4], [5]. Thus, the accomplishment of certain performance levels (i.e. collapse prevention, life safety, immediate occupancy, fully operational) [6], poses modern challenges for seismic design in terms of accurate structural analysis prediction and material innovation. In this scenario, in order to optimize the global response of the building, recent design processes benefit from resistance reserves in non-structural members [7], evaluating to what extent the performance of architectural elements enhances dynamic dissipation and faces the collapses. Moreover, as recent earthquakes have highlighted, non-structural components represent the higher percentage in cost reparation [8], although to date scarce information has been collected on the dynamic design of architectural members. In this light, the present paper illustrates the outcomes obtained through advanced numerical simulation of high-rise moment resisting frames (MRFs): glazed curtain wall stick systems were tested to calibrate equivalent nonlinear FE models, showing the overall influence of façades on structural frame seismic response. Since the analyses led to a novel insight on the external cladding dissipation properties, a step back to the design phase was conducted: taking advantage from smart materials, an innovative façade prototype was studied, aimed to enhance local and global seismic performance. Shape memory alloys (SMAs) opened a new path for the development of an intelligent manufacturing fashion, constituted by unique mechanical properties as shape memory

Open Science Index, Architectural and Environmental Engineering Vol:11, No:4, 2017 publications.waset.org/10006834.pdf

effect and superelasticity. However, although exploited in many fields from robotics to aerospace, today, research in SMA non-structural civil engineering applications is scarce.

II. Nonlinear Dynamic Analyses

Nonlinear time history analyses (NLTHa) were performed to predict the seismic behavior of the investigated structural prototypes: due to its intrinsic limitations [9], [10], pushover analyses present specific deficiencies in high-rise MRFs structural design, making nonlinear dynamic analysis the most attractive tool to determine robust solutions. Considering that various mechanical and physical idealizations were involved in façade-to-structure interaction, diversified modeling approaches were applied. Initially, a fiber-based FE model of the bare MRFs was implemented [11] on a open-source platform, investigating both the global and the local seismic performance of the structures. Subsequently, three-dimensional solid-based façade numerical models were developed to reproduce the complex phenomena underpinning the mechanics, i.e. assessing the aluminium frame deformability, the glass-to-frame interaction, the gasket mechanical distortion and the transom-to-mullion connection stiffness. Thus, laboratory test results [12] were emulated by numerical simulations, and equivalent mono-dimensional nonlinear link elements were calibrate to reflect the stress-to-strain curtain wall response in light of a computational time-saving approach. Consequently, plastic SMA actuators were designed through a validated parametric campaign of FEM analyses, in order to enhance the dissipating performance of the façade exploiting the peculiar properties of the SMA. Again, equivalent mono-dimensional nonlinear link elements were calibrate to reproduce the dynamic behaviour of the re-designed cladding. On one hand, detailed brick-based FE models gave more knowledge on the complex phenomena supporting the mechanics [13], [14], and replicating the local stress-to-strain response. On the other hand, calibrated links permitted to scale the complex simulation into classical fiber-based FE models, saving significant computational time. Finally, mono-dimensional façade links were implemented into the MRFs model.

A. Description of the Case-Study Buildings

Two 6 x 6-bay prototypes were extracted from reference thirty- and sixty-storey three-dimensional buildings, respectively named MF-01 and MF-02, designed in accordance with current European seismic standards [15] and considering high seismicity (i.e. PGA = 0.40 g) on soil class C (i.e. 180 m/s $<$ Vs $<$ 360 m/s). As shown in Fig. 1, where a sketch of plan is provided, the lateral-force resisting system (LFRS) was constituted by a central 5.6 x 5.6m braced core, connected with HD columns and perimetral CBF through orthogonal outrigger arms, placed every fifteen stories to limit inter-storey drifts and second order effects. External belt trusses rang the structure.

The external view and the chosen geometries are summarized in Fig. 2: The inter-storey height was designed to 3.3m, resulting in an overall height of 99m in MF-01

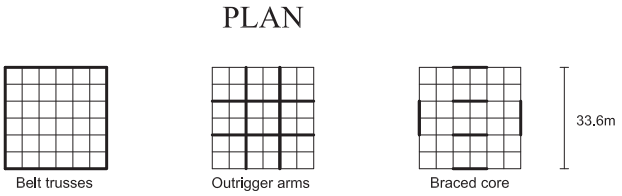

Fig. 1 Schematic of plan of the reference structures

and 198m MF-02. Uniform column spacing on the in-plane principal directions was set to 5.6m. Dead and live loads were considered to be 2kN/m^2 and 4kN/m^2, respectively, added to permanent non-structural internal weight. According to ASCE-7-05 provisions [16], the lateral wind pressure was calculated considering the speed at the ground equal to 37 m/s (84 mph).

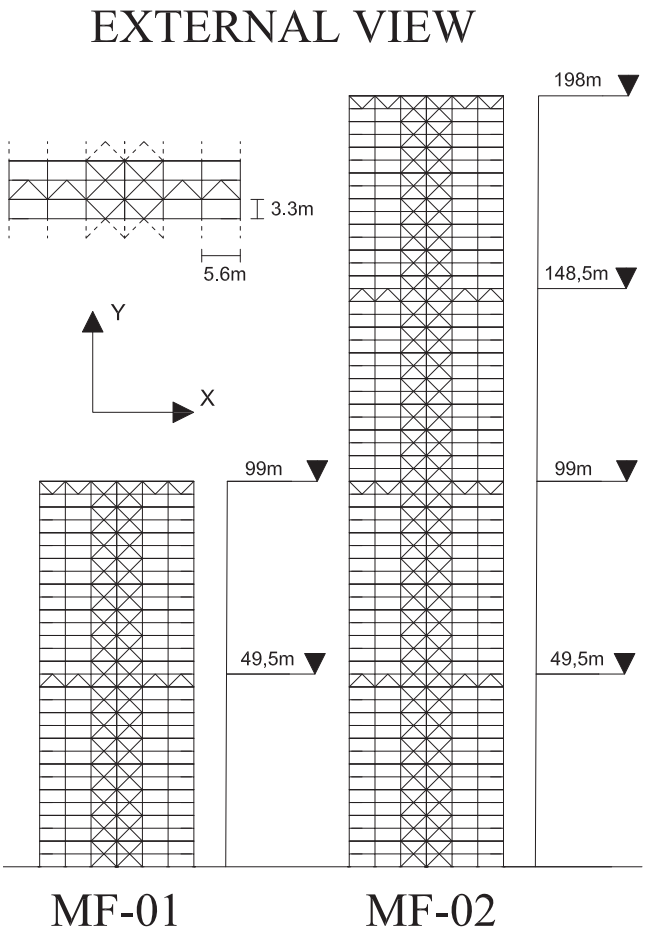

Fig. 2 Schematic of elevation of the reference planar frames

A series of response spectrum analyses (RSAs) were performed in SAP2000 [17] as first-stage design, considering medium ductility class (DCM) and the behaviour factor (q) for V bracing systems conservatively equal to 2, as specified in EC8 prescriptions [16] and according to [11]. Both brace and column sizes were assumed to be tapered along the height of the structure, while steel grade S-275, S450 and S700 were used for beams, columns and braces, respectively. Table I

summarises the dimensioning performed in accordance with [18].

TABLE I
DESIGNED GEOMETRY OF KEY STRUCTURAL COMPONENTS

	30-storey frames		**60-storey frames**	
	floor	*profile*	*floor*	*profile*
	1-5	HD400x509	1-20	HD400x900
	6-10	HD400x421	21-30	HD400x634
Columns	11-15	HD400x237	31-40	HD400x509
	15-20	HD400x237	41-50	HD400x314
	21-30	HD400x237	51-60	HD400x237
Beams	1-30	IPE400	1-60	IPE400
Outrigger	15/30	HD400x314	15/30/45/60	HD400x314
	1-5	HSS300x16	1-10	HSS400x16
Braces	6-15	HSS250x16	11-20	HSS350x16
	16-30	HSS200x16	21-60	HSS250x16

These assumptions imposed the fundamental period (T1) to be equal to 1.75s for MF-01 and 4.16s for MF-02. Equivalent rigid links and partially-hinged connections were considered, both for gusset-to-brace and beam-to-column connections respectively, in concordance with [19], [20].

1) FE Fiber-Based MRFs Modelling Approach: Advanced plastic force-based fiber element models were implemented on the open-source platform OpenSees [21], in order to analyze local and global seismic response of the MF-01 and MF-02 reference structures. The conceptual modeling was performed as detailed in Brunesi et al. [11], [18], subjecting the MRFs to NLTHAs deriving from a set of ten natural records [22], [23]. These accelerograms were spectrum-compatible in displacement according to EC8 prescriptions [15], selected a Type 1 spectrum with PGA=0.4g, soil Type C and T_D=8s.

B. Description of the Test Performed on the Commercial Stick Curtain Wall

Experimental data was achieved by full-size in-plane crescendo tests [12], conducted at the laboratory of the Construction Tecnologies Institute (ITC) of the Italian National Research Council (CNR), where a commercial full-scale stick curtain wall (Fig. 3) was assumed as a reference for the seismic response, once assessed the result integrity in concordance with [24]-[27]. Referring to Caterino et al. [12], the experimental set up consisted in a 5720 x 7370 mm steel frame, where three rigid beams was installed at different height acting as the principal structure slabs. Horizontal displacements could be imposed to the rigid beams simulating seismic-induced lateral drifts [29], [30].

Consistently with the designed MRF structure geometries, the tested façade was 7200 mm high and 5600 mm wide, with 3300 mm inter-storey height. The test unit had six transoms and five mullions with different cross-section profile: the external transoms had a lower inertia respect to the other spans. The commercial aluminium alloy adopted for the members was EN-AW 6060-T6. The insulated glazing panel thickness was 8+8.2+16+6mm, constituted by a tempered glass of E = 70 GPa. A U-shaped steel joint connected the alluminium transoms with the mullions, while internal and external silicone gasket layers were settled along the contact edges to support the glass panel, with a clearance of 5 mm.

1) FE Three-Dimensional Façade Modelling Approach: According to [12], four parameters were accredited as main responsible of the lateral response of the façade: (i) the aluminium frame geometry and the transom-to-mullion joint rotational stiffness; (ii) the clearance between glass panels and the aluminium frame; (iii) the mechanical behavior of gaskets; (iv) the local interaction when contact occur between glass and frame [27]-[29]. Three-dimensional brick-based models were developed in ABAQUS 6.14 [30] to interpret local mechanics and interactions between each parameter (i-iv). Thus, equivalent nonlinear connector elements were calibrated to explicitly reproduce the rotational stiffness of transom-to-mullion connection (Fig. 4) and glass-to-gaskets slippage (Fig. 5), accounting for potential impacts between the glazed surface and the aluminium frame.

In line with a computational time-saving approach [31], [32], these connectors were implemented on a full-scale model, reducing the amount of mesh elements and the internal variables, in order to reproduce the global tested response (Fig. 6). Three-dimensional deformable isoparametric elements constituted by 8-node linear bricks were adopted to model the connections, accounting for finite strain and rotation in large-displacement analysis. Both geometrical and material nonlinearities were considered. Standard rate-independent Von Mises model associated to yield surface for isotropic materials and strain hardening was assumed, reproducing the classical cyclic stress-to-strain low during the applied loading-unloading history. According to Memari et al. [32], an equivalent full-section glass panel was considered, adopting isotropic elastic three-dimensional elements (C3D8R) and evaluating the maximum stress response at local scale. The mechanical strain of the gasket and the glass-to-gasket nonlinear friction effect due to the frame deformation were modeled by an equivalent stress-strain constitutive law, deducted in accordance with [32]-[34] and through the experimental tests carried out at the Institute of Construction Technology. Since numerous in-plane racking tests [26], [31], [32] have demonstrated that glass cracks propagate when glass-to-frame contact occurs in corners, a stiffening increment was considered after the impact.

C. Dissipative Improvements through Designed SMA Actuators

Although the nickel-titanium alloy original formula was developed by Buchler and Wiley [35] in 1960s, crucial improvements have been produced by researchers, maintaining the well-known peculiar properties and lending it to innovative applications and devices. The most recognised mechanical behaviours are the shape memory effect and the superelasticity. The first property reflects the ability to recover the original shape of severely deformed specimens after a thermal cycle. The second permits, at high temperatures, to restore the initial configuration after being intensely deformed through mechanical loading-unloading cycle executed at constant temperature [36]. The amount of industrial applications is growing year by year, as highlighted by the overall annual growth rate estimated to be 12.8% between 2011 and 2016

Open Science Index, Architectural and Environmental Engineering Vol:11, No:4, 2017 publications.waset.org/10006834.pdf

Open Science Index, Architectural and Environmental Engineering Vol:11, No:4, 2017 publications.waset.org/10006834.pdf

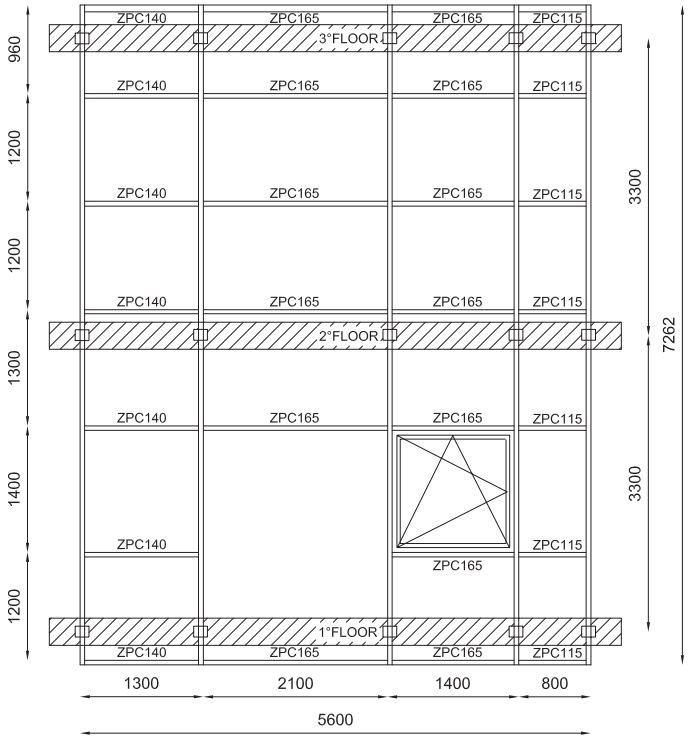

Fig. 3 Tested façade geometry. Note: dimensions in mm

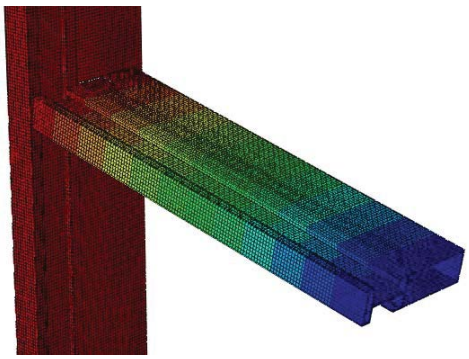

Fig. 4 3D modelling of the transom-to-mullion connection

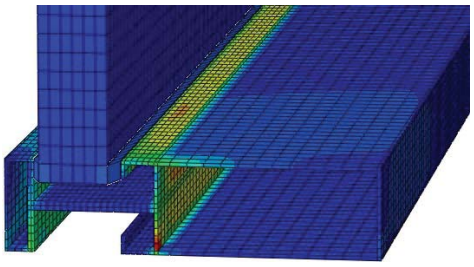

Fig. 5 3D modelling of the glass-to-gasket connection

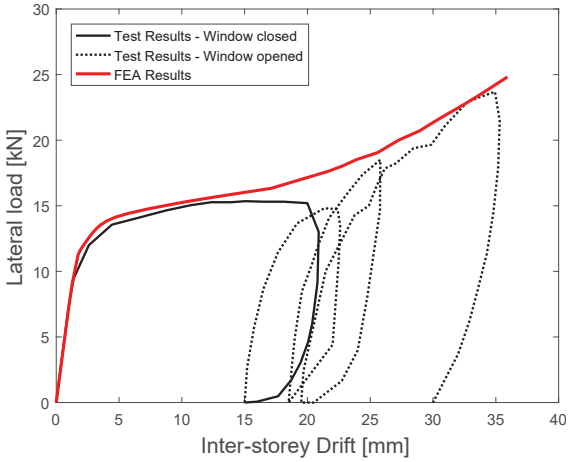

Fig. 6 FEA and force-displacement results of tested façade

[37]. SMAs demonstrated their decisive role in smart device design, providing potential self-adapting and self-sensing properties, acting as actuators and monitoring the structure functionality. In particular, decisive interest has been allocated to seismic dissipation in civil engineering applications, investigating engineered prototypes able to reduce earthquake shaking actions [38], [39]. The usual concept underpinning SMA isolation devices is to affect the structural response applying special components directly to the structural frame [40]. Traditional devices should: transmit vertical loads; limit the base shear forces; provide the optimal lateral stiffness; absorb most of the structural displacement demand; provide an adequate initial stiffness and strength to make the isolation system rigid under service loads; reduce the residual displacements; and permit easy component replacement [41]. The innovative nature of this paper is to provide an alternative source of seismic dissipation directly applying thin SMA elements on nonstructural members, supporting the hysteretic damping of the classical isolation systems. Researches have

Open Science Index, Architectural and Environmental Engineering Vol:11, No:4, 2017 publications.waset.org/10006834.pdf

emphasized the growing need for nonstructural elements seismic enhancement, especially in critical facilities, in order to maintain fully-operational conditions after the earthquake event and reducing the damage as well [42].

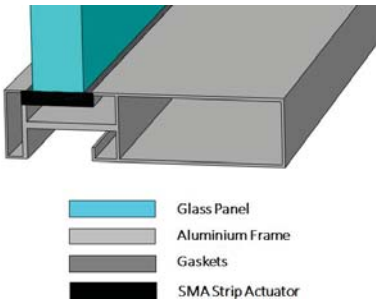

Fig. 7 3D modelling of SMA strip actuators

The novelty of this work consists in design smart glazed façades, opening the engineering market to new sources of dissipation. Since mullion-to-transom and glass-to-gasket modelling (Figs. 4 and 5) highlighted that the glass slippage controlled the global behaviour, regulated by the mechanical distortion of the gasket and the frame-to-glass clearance, SMA actuators were installed to govern these parameters through energy dissipation capabilities. Fig. 7 displays the theoretical model of the glazed curtain wall stick system, where the glass panel, the aluminium frame and the SMA elements are defined. Through a validated parametric campaign of FEM analyses, geometric and mechanical prototype details were investigated, making SMAs the ideal material in innovative nonstructural isolation technologies due to: (i) large elastic strain capacity, (ii) hysteretic damping, (iii) good high- and low-cycle fatigue resistance, (iv) recentering capabilities, (v) excellent thermal and corrosion resistance, (vi) shape memory effect in case of temperature leap [37]. The actuators were designed to be easily fixed to the traditional façade. Table II summarizes the adopted parameters, implemented in ABAQUS through the UMAT subroutine for superelasticity and plasticity of shape memory alloys [30].

TABLE II
SHAPE MEMORY ALLOY SELECTED PROPERTIES

DESCRIPTION	*VALUE*
Austenite Elasticity	50000 [MPa]
Austenite Poisson's Ratio	0.33
Martensite Elasticity	45000 [MPa]
Martensite Poisson's Ratio	0.33
Trransformation Strain	0.05
Start of Transformation Loading	380 [MPa]
End of Transformation Loading	490 [MPa]
Reference Temperature	22 [°C]
Start of Transformation Unloading	220 [MPa]
End of Transformation Unloading	120 [MPa]
Ultimate stress-strain point	975 [MPa], 0.15

III. RESULTS AND COMPARISONS

In the following, the main results obtained for the two reference high-rise structures MF-01 and MF-02 will be summarised in terms of NLTHa global and local performance. In particular, the influence of thin shape memory alloy strip actuators applied on glazed curtain wall system will be displayed, illustrating to which extent these affect the overall seismic response. Initially, the comparison between NLTHa average response carried out from the structures with glazed curtain walls (NLTHA Avg on diagrams), respect to the correspondent structures with SMA modified façades (SMA ACTUATOR on diagrams) will be shown. Consequently, the percentage variation between the two components will be provided. Individual earthquake (EQs) acceleration results, referred to the MRF with glazed curtain walls elements, will be depicted in grey.

A. Global Performance

Fig. 8 displays the global response of the two mega-frame buildings in terms of peak floor acceleration, respectively for MF-01 and MF-02. NTHAs were performed on the structures, both with the innovative system (hereinafter called SMA-façades) and on the high-rise MRF with traditional façades (hereinafter called SMA-façades): average and individual (EQs) earthquake record results are depicted below.

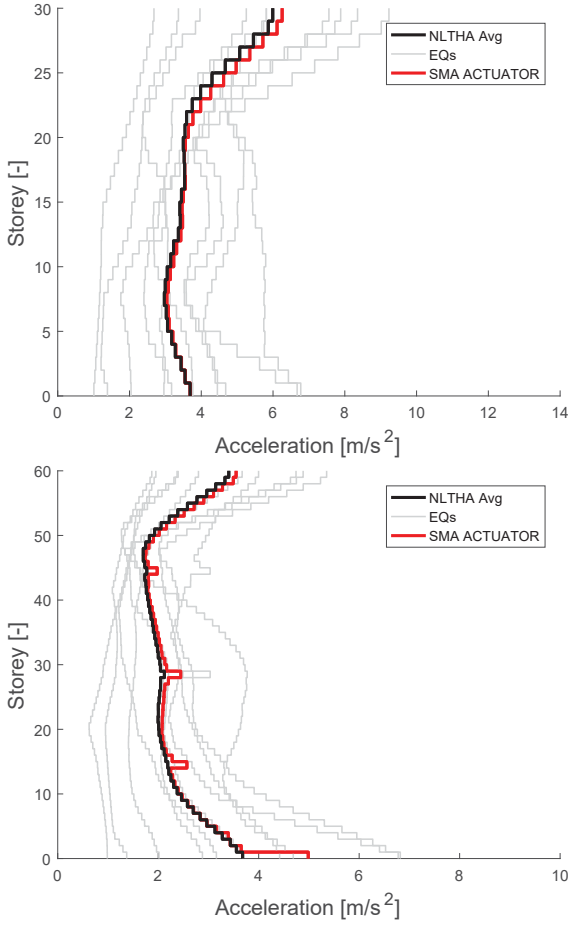

Fig. 8 Acceleration profile in MF-01 and MF-02

Assembling thin shape memory alloy actuators on the glazing curtain wall systems, the structures gain in stiffness moderately, as highlighted by modest floor acceleration increments.

Open Science Index, Architectural and Environmental Engineering Vol:11, No:4, 2017 publications.waset.org/10006834.pdf

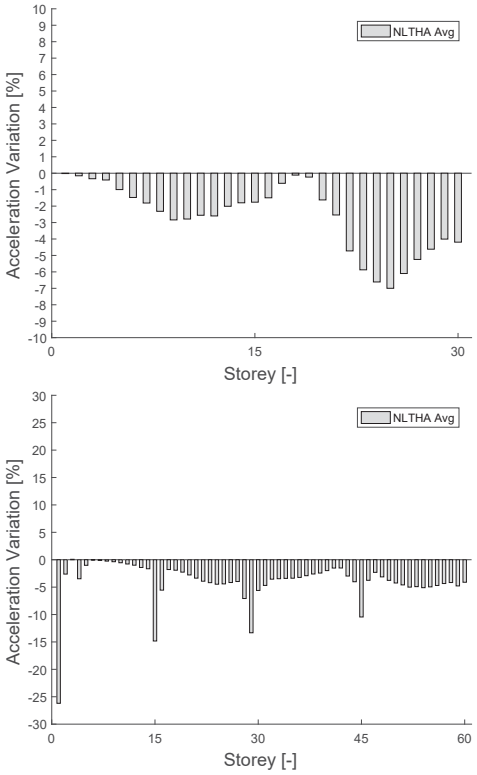

Fig. 9 Acceleration profile percentage variation in MF-01 and MF-02

Peak accelerations, achieved in the most extreme records, were 0.92 g and 0.68 g, while medium values up to 0.61 g and 0.52 g were obtained. Fig. 9 summarises the percentage variation between performance results, i.e. between the average response of the MRF with traditional external cladding and the response enhanced by SMA actuators. In MF-01 the discrepancies rose up to 7%, whereas in MF-02 the response assumed greater variations (up to 26%) with peaks in correspondence to the outrigger. According to [11], [18] this aspect denotes the stiffening effect provided by the outriggers, as evidenced by a pronounced reduction in terms of peak inter-storey drifts. Although the façade dissipating behaviour tends to influence the overall acceleration response, mitigating the peaks on the outrigger floors, SMA-façades provide an additional post-yielding contribute in stiffness causing potential matches between individual earthquake record and structural frequencies, emerging into possible resonance phenomena that led to amplified local response. Fig. 10 underlines the global response of the two mega-frame buildings in terms of peak displacement, together with their average values, respectively for MF-01 and MF-02. Peak displacements, achieved in the most extreme records, were 0.58 m and 1.81 m, while medium values up to 0.48 m and 0.94 m were obtained. According to Brunesi et al. [11], [18], the response assumed a rough cantilevered shape.

Fig. 11 summarises the percentage variation between traditional- and SMA-façades, highlighting that both in MF-01 and MF-02 actuators amplified the average displacement in the lower floors (approximately 1/4 of the structural height), while the displacement were reduced up to 3% in the others

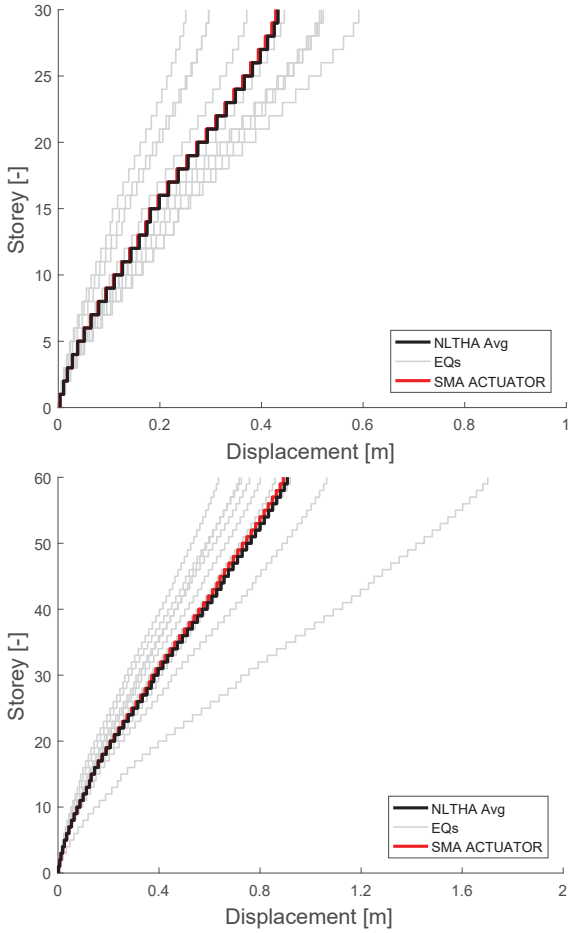

Fig. 10 Displacement profile in MF-01 and MF-02

toward the top, i.e. where the structural displacement reaches its maximum.

B. Local Performance

As stated during the design phase and according to [11], [18], the key members delegated to resist to the major earthquake-induced stresses in the adopted LFRS are the core braces. NLTHA response in term of axial load peak profiles in critical components will be shown, correlated to the percentage variation computed between traditional- and SMA-façades results. Moreover, Fig. 12 demonstrates that braces mostly supported dynamic effects: in fact, the static-to-dynamic proportion is depicted in the most critical brace for both the high-rise buildings, while Fig. 13 shows the same rate in most critical columns. Comparing the diagrams is evidenced that the principal dynamic-induced compressive demand (in ratio) were slightly more pronounced in braces than those evidenced in columns, thus only the compression percentage variations in braces will be displayed.

Pronounced discontinuities were again predicted in correspondence to the outriggers. Seismic axial loads of up to 4600 kN and 4800 kN were obtained in braces, respectively for MF-01 and MF-02. As highlighted in Figs. 12 and 14, a similar demand was achieved in correspondence to the ground level and to the mid-height outrigger floor,

Open Science Index, Architectural and Environmental Engineering Vol:11, No:4, 2017 publications.waset.org/10006834.pdf

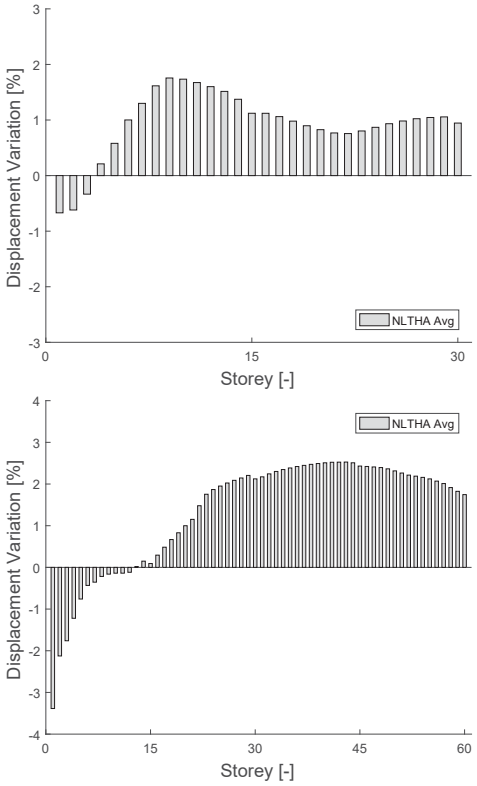

Fig. 11 Displacement profile percentage variation in MF-01 and MF-02

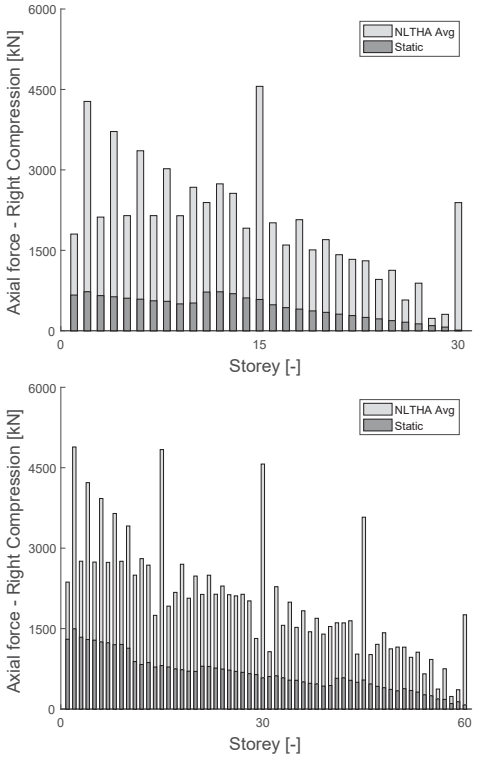

Fig. 12 Static-to-seismic axial load ratios in braces

reflecting the storey acceleration trend depicted in Fig. 8, prorated according to the floor masses. Fig. 15 displays the compression percentage variation in key braces. In this case, it is clearly underlined that SMA actuators positively affect the seismic response when the structural height increase, i.e. mostly reducing the stresses on the LRFS members. However, although in MF-01 the discrepancy between traditional- and SMA-façades results apparently do not led to a pronounced behaviour in favor or against the adoption of actuators, the diagram suggests that where the most extreme axial load were collected, SMA-façades better unload the critical members (up to 11.2%).

IV. Conclusion

The main considerations acquired from the NLTHA comparisons are herein synthesized:

- Effects caused by façade dissipation were proven to be not negligibly on the global response: thin SMA actuators reduced up to 3% of top displacement.
- Façade with SMA strips unloaded critical LRFS braces up to 11.2% of axial stress.
- Sensitivity to the structural height was investigated, showing that shape memory alloys mainly influenced the response with a reverse trend respect to the height.

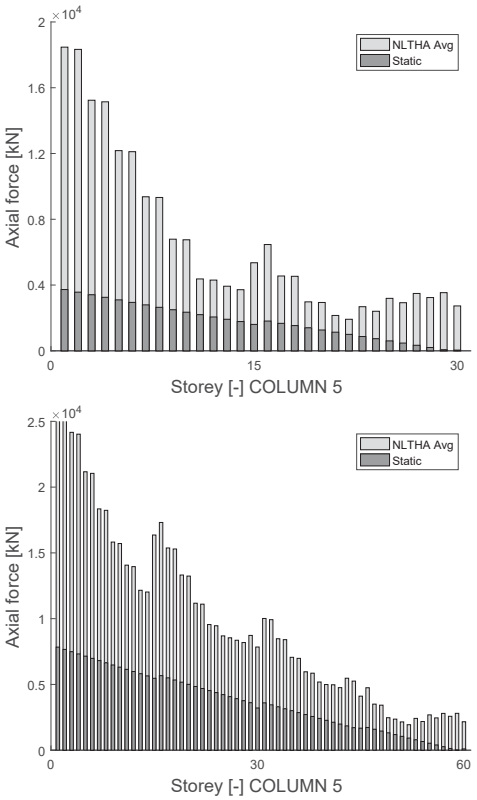

Fig. 13 Static-to-seismic axial load ratios in columns

Open Science Index, Architectural and Environmental Engineering Vol:11, No:4, 2017 publications.waset.org/10006834.pdf

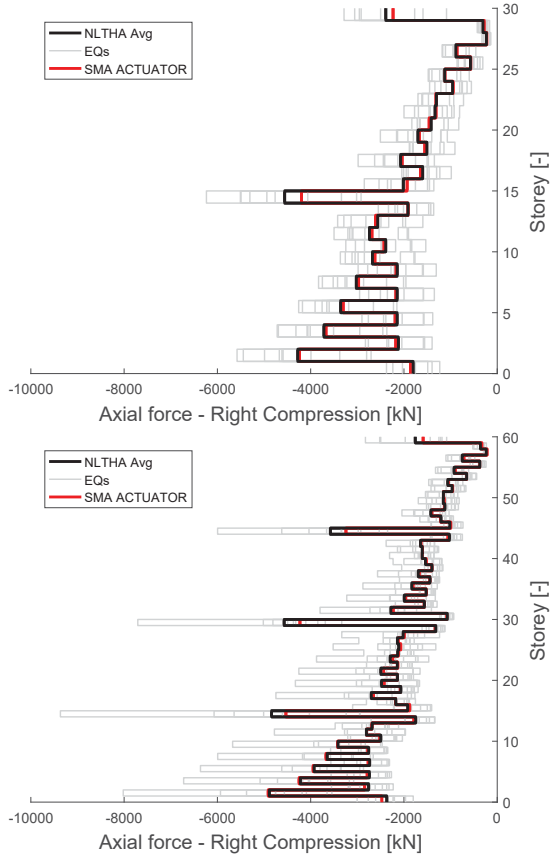

Fig. 14 Axial load brace profile in MF-01 and MF-02

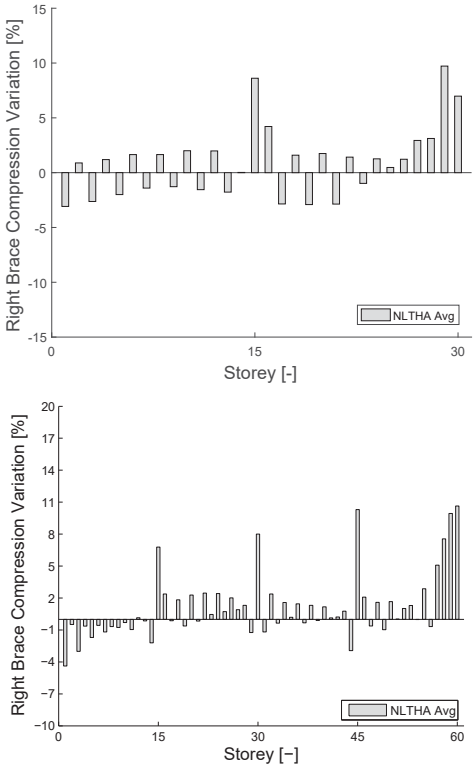

Fig. 15 Brace percentage variation in MF-01 and MF-02

ACKNOWLEDGMENT

The authors would like to thank Miss Jessica Sisinni, M. Sc. candidate in Civil Engineering - University of Pavia, for her dedication in three-dimensional FE façade modelling.

REFERENCES

[1] H. Fan, Q.S. Li, A.Y. Tuan, L. Xu, *Seismic analysis of the worlds tallest building*, J Constr Steel Res. 2009,65, 1206-15.

[2] X. Lu, X. Lu, H. Guan, W. Zhang, L. Ye, *Earthquake-induced collapse simulation of a super-tall mega-braced frame-core tube building*, J Constr Steel Res. 2013,82, 59-71.

[3] X. Lu, X. Lu, H. Sezen, L. Ye, *Development of a simplified model and seismic energy dissipation in a super-tall building*, Eng Struct. 2014,67, 109-22.

[4] G.M. Montuori, E. Mele, G. Brandonisio, A. De luca, *Secondary bracing systems for diagrid structures in tall buildings*, Eng Struct. 2014,75, 477-88.

[5] G.M. Montuori, E. Mele, G. Brandonisio, A. Deluca, *Design criteria for diagrid tall buildings: stiffness versus strength*, Struct Des Tall Build. 2014,23, 1294-314.

[6] R.O. Hamburger, *Performance-Based Analysis and Design Procedure for Moment Resisting Steel Frames*, Background Document, SAC Steel Proj. Sept. 1998.

[7] A. Filiatrault and T. Sullivan, *Performance-based seismic design of nonstructural building components: The next frontier of earthquake engineering*, Earthq Eng & Eng Vib. 2014,13:17-46.

[8] E. Miranda and S. Taghavi, *Estimation of Seismic Demands on Acceleration-sensitive Nonstructural Components in Critical Facilities*, Seminar ATC29-2. 2003,347-360.

[9] H. Krawinkler, G.D.P.K. Seneviratna, *Pros and cons of pushover analysis of seismic performance evaluation*, Eng Struct. 1998,20, 452-62.

[10] A.K. Chopra, R.K. Goel, *A modal pushover analysis procedure to estimate seismic demand for unsymmetric-plan buildings*, Earthquake Eng Struc Dyn. 2004,33, 903-27.

[11] E. Brunesi, R. Nascimbene, L. Casagrande , *Seismic analysis of high-rise mega-braced frame-core buildings*, Eng Struct. 2016,115, 1-17.

[12] N. Caterino, M. DelZoppo, G. Maddaloni, A. Bonati, G. Cavanna, A. Occhiuzzi, *Seismic assessment and finite element modelling of glazed curtain walls*, Struct Eng Mech. 2017,61(1), 77-90.

[13] R. Nascimbene, G.A. Rassati, K.K. Wijesundara, *Numerical simulation of gusset-plate connections with rectangular hollow section shape brace under quasi-static cyclic loading*, J Constr Steel Res. 2011,70, 177-79.

[14] E. Brunesi, R. Nascimbene, M. Pagani, D. Belic, *Seismic performance of storage steel tanks during the May 2012 Emilia, Italy, earthquakes*, J Perform Constr Facil ASCE. 2015, 29(5),04014137.

[15] *Eurocode8. Design of structures for earthquake resistance-Part1: General rules,seismic actions and rules for buildings*, EN 1998-1-1. Brussels (Belgium) 2005.

[16] *ASCE7-05. Minimum design loads for buildings and other structures*, Reston(VA):American Society of Civil Engineers 2006.

[17] *SAP2000. Linear and nonlinear static and dynamic analysis and design of three-dimensional structures*, Berkeley (CA): Computers and Structures Inc. (CSI).

[18] E. Brunesi, R. Nascimbene, G.A. Rassati, L. Casagrande , *Seismic performance of highrise steel MRFs with outrigger and belt trusses through nonlinear dynamic FE simulations*, Seminar COMPDYN2015, 5th ECCOMAS. 2015.

[19] R. Nascimbene, G.A. Rassati, K.K. Wijesundara, *Numerical simulation of gusset-plate connections with rectangular hollow section shape brace under quasi-static cyclic loading*, J Constr Steel Res. 2011,70, 177-79.

[20] E. Brunesi, R. Nascimbene, G.A. Rassati, *Seismic response of MRFs with partially-restrained bolted beam-to-column connections through FE analyses*, J Constr Steel Res. 2015,107, 37-49.

[21] *OpenSees. Open system for earthquake engineering simulation*, Berkeley (CA): Pacic Earthquake Engineering Research Center, University of California.

[22] T.J. Sullivan, *Direct displacement-based seismic design of steel eccentrically braced frame structures*, Bull Earthq Eng. 2013,11, 2197-231.

[23] T.J. Maley, R. Roldán, A. Lago, T.J. Sullivan, *Effects of response spectrum shape on the response of steel frame and frame-wall structures*, Pavia (Italy): IUSS Press. 2012.

[24] S.J. Thurston, A.B. King, *Two-directional cyclic racking of corner curtain wall glazing*, Building Research Association of New Zeland (BRANZ). 1992.
[25] C.P. Pantelides, R.A. Behr, *Dynamic in-plane racking tests of curtain wall glass elements*, Earthquake Eng Struc. 1994,23(2), 211-228.
[26] R.A. Behr, A. Belarbi, J.H. Culp, *Dynamic racking tests of curtain wall glass elements with in-plane and out-of-plane motions*, Earthquake Eng Struc. 1995b,24(1), 1-14.
[27] R.A. Behr, *Seismic performance of architectural glass in mid-rise curtain wall*,JArchEng. 1998,4(3), 94-98.
[28] J.G. Bouwkamp, J.F. Meehan, *Drift limitations imposed by glass*, Proceedings of the Second World Conference on Earthquake Engineering, Tokyo, Japan. 1960.
[29] J.G. Bouwkamp, *Behavior of windows panels under in-plane forces*, B Seismol Soc Am. 1961,51.1, 85-109.
[30] *ABAQUS 6.14 Documentation, Dassault Systmes Simulia Corp*, Providence, RI, USA. 2016
[31] S. Sivanerupan, J.L. Wilson, E.F. Gad, N.T.K. Lam, *Seismic Assessment of Glazed Façade Systems*, Proceedings of the Annual Technical Conference of the Australian Earthquake Engineering Society, Newcastle. 2009.
[32] A.M. Memari, A. Shirazi, P.A. Kremer, *Static finite element analysis of architectural glass curtain walls under in-plane loads and corresponding full-scale test*, Struct Eng Mech. 2007,25(4),365-382.
[33] J. Kimberlain, L. Carbary, C.D. Clift, P. Hutley, *Advanced Structural Silicone Glazing*, International J High-Rise Buil. 2013, 2(4), 345-354.
[34] W. Lu, B. Huang, K.M. Mosalam, S. Chen, *Experimental evaluation of a glass curtain wall of a tall building*, Earthquake Eng Struct. 2016, 45, 1185-1205.
[35] W.J. Buehler and R.C. Wiley, *Nickel-based alloys*, Technical report, US-Patent 3174851. 1965.
[36] F. Auricchio, L. Taylor, J. Lubliner, *Shape-memory alloys: macromodelling and numerical simulations of the superelastic behavior*,Comput Methods Appl Mech Engeg. 1997,146,281-312.
[37] C. Menna, F. Auricchio, D. Asprone, *Applications of Shape Memory Alloys in Structural Engineering*, L. Concilio, A. Lecce (Eds.), Shape memory alloy engineering, Butterworth-Heinemann, Boston. 2015, pp. 369403 [chapter 13].
[38] G. Attanasi and F. Auricchio, *Innovative superelastic isolation device*, J Earthquake Eng. 2011, Volume 15-S1,72-89.
[39] A. Nespoli, D. Rigamonti, M. Riva, E. Villa, F. Passaretti, *Study of pseudoelastic system for the design of complex passive dampers: static analysis and modeling*, Smart Mater Struct. 2016, 25,105001.
[40] J. McCormick, R. Desroches, D. Fugazza, F. Auricchio, *Seismic assessment of concentrically braced steel frames with shape memory alloy braces*, J Struct Eng. 2007,133,862-870.
[41] C. Christopoulos, A. Filiatrault,*Review of Principles of Passive Supplemental Damping and Seismic Isolation*, IUSS Press, Pavia. 2006,88-7358-037-8.
[42] B.S. Ju, A. Gupta, Y.H. Ryu,*Piping Fragility Evaluation: Interaction With High-Rise Building Performance*, J. Pressure Vessel Technol. 2016,139(3),031801.

Open Science Index, Architectural and Environmental Engineering Vol:11, No:4, 2017 publications.waset.org/10006834.pdf